u = velocity
u_c = velocity at center of pipe
$\bar{u}$ = average velocity
x = distance along pipe
y = distance from pipe wall

Greek Letters

β = mass flow ratio
δ = volume flow ratio
γ = ratio of specific heats
ν = kinematic viscosity
ρ = density
τ_w = wall shear stress
μ = dynamic viscosity

Subscripts

g = gas phase
l = liquid phase

Superscript

* = critical conditions for which $N_M = \gamma^{-1/2}$

LITERATURE CITED

1. Mottard, E. J., and C. J. Shoemaker, *Natl. Aeronaut. Space Admin. Tech. Note D-991* (1961).
2. Tangren, R. F., C. H. Dodge, and H. S. Seifert, *J. Appl. Phys.*, **20**, No. 7, 637-645 (1949).
3. Muir, J. F., and R. Eichhorn, *Proc. Heat Trans. Fluid Mech. Inst., Stanford,* 183-204 (1963).
4. Campbell, I. J., and A. S. Pitcher, *Proc. Roy. Soc. London,* **243A**, 534-545 (1957).
5. Zuber, N., *J. Heat Transfer,* **82C**, 255-258 (1960).
6. Levy, S., *J. Heat Transfer,* **85C**, 137-152 (1963).
7. Woodbury, S. P., M.E. thesis, Univ. New South Wales, in preparation.
8. Hsieh, D. Y., and M. S. Plesset, *Phys. Fluids,* 4, No. 8, 970-975 (1961).
9. Schlichting, H., "Boundary Layer Theory," 4 ed., McGraw-Hill, New York.
10. James, W., and E. Silberman, *St. Anthony Falls Hydraulic Lab. Tech. Paper No. 26,* Ser. B, Univ. Minnesota.
11. Alves, G. E., *Chem. Eng. Progr.,* **50**, No. 9, 449-459 (1954).

Manuscript received March 2, 1966; revision received June 17, 1966; paper accepted June 22, 1966.

Stability of a Fluid in a Rectangular Region Heated from Below

MICHAEL R. SAMUELS and STUART W. CHURCHILL

University of Michigan, Ann Arbor, Michigan

Finite-difference methods were used to compute hydrodynamic instability due to natural convection in an enclosed horizontal rectangular region heated from below. Critical Rayleigh numbers were determined for a series of Prandtl numbers and length-to-height ratios. For Prandtl numbers greater than unity excellent agreement was obtained between these calculations and the values predicted by Kurzweg on the basis of a linearized theory. However, for Prandtl numbers less than unity the critical Rayleigh numbers exhibited a dependence on N_{Pr}, which was not predicted by the linearized theory. For Rayleigh numbers greater than the critical, complete temperature and velocity fields were determined.

The calculations assumed that the fluid motion is two dimensional. Experiments have indicated that the flow may be two or three dimensional depending on minor perturbations in the boundary conditions.

Although a number of metastable two-dimensional circulations are possible for symmetrical initial conditions, the calculation always converged to a single, unique solution for any asymmetric initial condition.

Situations in which a small perturbation can cause complete rearrangement of the system are termed *unstable.* Such situations are of special interest to engineers, since an instability may pose difficulties in design and operation.

Natural convection can be described by the equations of conservation of mass, energy, and momentum. Analytical solutions for these coupled, partial differential equations are difficult, if not impossible, to obtain except for very idealized cases. However, the use of finite-difference techniques has led to solutions for a number of important problems (*1, 2, 6, 19*).

The objective of this work was to demonstrate the usefulness of finite-difference techniques in the study and characterization of unstable systems. In particular, instability due to natural convection in an enclosed, horizontal region of rectangular cross section heated from below was studied.

HISTORICAL BACKGROUND

The first reference to the existence of natural convection between horizontal plates heated from below appears to be by Thomson (*18*), who in 1882 noted the presence of cellular patterns in soapy water whose mean temperature was greater than ambient. In 1900, Bénard (*3*) published photographs taken with a beam of parallel light which had passed through a layer of paraffin oil whose thickness was small compared with its diameter and which was heated from below. These photographs clearly indicated the presence of a hexagonal cellular convection pattern. [There is recent evidence (*17*) that the cells observed by Thompson and Bénard were caused by surface tension, rather than thermal gradients. However, the effects of surface tension can apply only in studies where the upper surface is free; they are not encountered in enclosed regions.]

In 1916 Lord Rayleigh (*13*) set forth the basic approach to the analytical treatment of convective instability in an enclosed infinite region heated from below. He linearized the equations of motion by assuming that all second-order perturbations of the pure conduction solution could be discarded, and he accounted for the cellular behavior observed by Bénard by assuming a solution for the velocity and temperature perturbations in terms of Fourier series. For the unrealistic case of no shear along the upper and lower boundaries he was able to calculate the critical temperature difference below which pure conduction was stable.

A complete solution for the linearized equations of motion with either free or fixed boundary conditions on the upper or lower surface was presented by Pellew and Southwell (*11*) in 1940. Because of the linearization of the equations of motion, the hexagonal cell observed by Bénard could not be explained, nor could heat transfer rates be determined.

Recently, much effort has been expended in an effort to explain the hexagonal cells of Bénard and to predict the rates of heat transfer in the presence of convective motion, but only partial success has been obtained.

The first experimental study of instability in a region with length-to-height ratio near unity appears to be that of Sorokin (*16*), who in 1961 studied natural convection in a long, horizontal cylinder of circular cross section heated from below. Observations of the paths of aluminum particles suspended in the working fluid indicated that two modes of convection were possible: a two-dimensional planar rotation with no component of velocity parallel to the axis of the cylinder, and a three-dimensional cellular pattern. For a Rayleigh number just above the critical value the two-dimensional mode was preferred, while for a Rayleigh number far above the critical value the three-dimensional mode was preferred.

In 1964 Deardoff (*5*) used finite-difference techniques to integrate the Navier-Stokes equations for two-dimensional, natural convection in an enclosed rectangular region heated from below. Length-to-height ratios of 1 to 1 and 2 to 1 were studied. Rayleigh numbers greater than 6.75×10^5 were investigated in an effort to describe turbulent convection. However, the assumption of two-dimensional motion was found to suppress the appearance of random fluctuations, and in most cases a nearly steady state solution was obtained.

In 1965 Kurzweg (*9*) developed a stability criterion for two-dimensional, natural convection in a horizontal enclosed rectangular region which is heated from below. The linearized equations of motion were assumed to have a solution for the temperature and stream function in the form of two infinite series of orthogonal functions. A modified Fourier technique, as outlined by Poots (*12*), was used to evaluate the values of the Rayleigh numbers for which nontrivial solutions exist. The lowest of these values is taken to be the critical Rayleigh number N_{Ra_c}. Values of N_{Ra_c} are presented for values of L/H from 0 to 4 to 1. The variation of $N_{\overline{Nu}}$ with N_{Ra} for N_{Ra} greater than N_{Ra_c} could not be determined by this method, and a dependence of N_{Ra_c} on N_{Pr} was not predicted.

In 1965 Aziz (*1*) presented the results of a numerical study of natural convection within a horizontal region of square cross section and within a cube. Results are presented for $N_{Pr} = 1.0$ and 7.0 in the range of $1{,}000 \leq N_{Ra} \leq 1{,}750$.

Fromm (*7*) recently presented the results of several numerical solutions for two-dimensional, natural convection in an enclosed rectangular region heated from below and subject to either no-shear or no-slip boundary conditions on the horizontal walls. Cyclic and no-slip conditions were postulated for the vertical walls. Results are presented for no-slip boundaries in a cell seven units long and three units high. Two-, three-, and four-celled patterns were forced to exist by using appropriate, symmetrical initial conditions. Apparently, the stability of these patterns to a general or unsymmetrical disturbance was not tested. Approximately equal heat fluxes were found with the different patterns at steady state.

MATHEMATICAL STATEMENT OF THE PROBLEM

In the calculations presented herein it will be assumed that the motion is two dimensional. This mode has been observed experimentally, and therefore the calculated results should have physical signficance. Whether a two- or three-dimensional motion is the more stable is, however, unknown. Fortunately, the lumped parameters, such as total heat flux, have almost equal values for two- and three-dimensional motions near the critical Rayleigh number. Indeed, it is just this similarity between the various modes which makes their relative stability so difficult to determine.

Three-dimensional calculations are theoretically feasible by an extension of the methods presented herein, but an increase of several orders of magnitude in computer time would be required.

Under the assumption of two-dimensional flow the problem may be described as follows.

A fluid of mean temperature θ_o is at rest within the rectangular region $0 \leq x \leq L$, $0 \leq y \leq H$ (see Figure 1). The fluid initially has a linear vertical temperature gradient with $\theta = \theta_i$ at the upper surface and $\theta = \theta_h$ at the lower surface. A small disturbance in velocity is introduced in the central region and allowed to develop until a steady

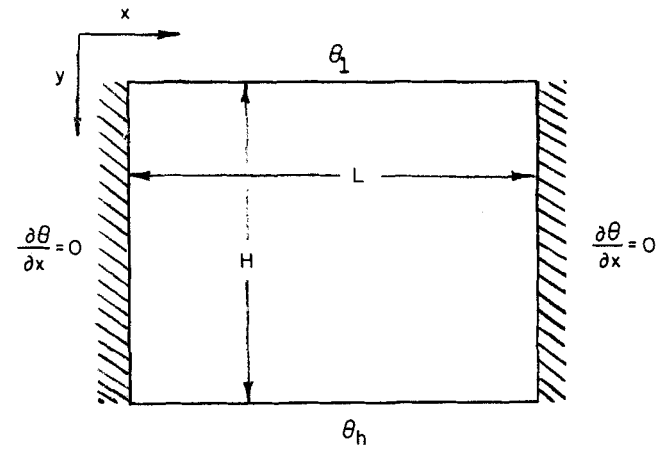

Fig. 1. The physical problem.

state convection pattern is established, or until all motion begins to die out.

The two-dimensional equations of motion for this problem may be written as follows:

Momentum:

$$\frac{\partial u}{\partial t} + u\frac{\partial u}{\partial x} + v\frac{\partial u}{\partial y} = -\frac{1}{\rho_o}\cdot\frac{\partial p}{\partial x} + \nu_o\left[\frac{\partial^2 u}{\partial x^2} + \frac{\partial^2 u}{\partial y^2}\right] \quad (1)$$

$$\frac{\partial v}{\partial t} + u\frac{\partial v}{\partial x} + v\frac{\partial v}{\partial y} = -\frac{1}{\rho_o}\cdot\frac{\partial p}{\partial y} + g\beta(\theta-\theta_o) + \nu_o\left[\frac{\partial^2 v}{\partial x^2} + \frac{\partial^2 v}{\partial y^2}\right] \quad (2)$$

Energy:

$$\frac{\partial \theta}{\partial t} + u\frac{\partial \theta}{\partial x} + v\frac{\partial \theta}{\partial y} = \kappa\left[\frac{\partial^2 \theta}{\partial x^2} + \frac{\partial^2 \theta}{\partial y^2}\right] \quad (3)$$

Continuity:

$$\frac{\partial u}{\partial x} + \frac{\partial v}{\partial y} = 0 \quad (4)$$

The initial and boundary conditions

$$\left.\begin{aligned} &u(x,y,0) = f_1(x,y)\\ &v(x,y,0) = f_2(x,y)\\ &\theta(x,y,0) = \theta_l + \frac{y}{H}(\theta_h - \theta_l)\\ &\theta(x,0,t) = \theta_l\\ &\theta(x,H,t) = \theta_h\\ &\frac{\partial\theta}{\partial x}(0,y,t) = \frac{\partial\theta}{\partial x}(L,y,t) = 0\\ &u = v = 0 \text{ on all surfaces.} \end{aligned}\right\} \quad (5)$$

then complete a formal statement of the problem. The above representation assumes that μ, k, and c_p are constants, and that variations of ρ are negligible, except as they affect the gravitational term. It is also assumed that $\beta(\theta_h - \theta_l) << 1$.

When one follows Hellums and Churchill (8), the above representation may be de-dimensionalized to

$$\frac{\partial U}{\partial \tau} + U\frac{\partial U}{\partial X} + V\frac{\partial U}{\partial Y} = -\frac{\partial P}{\partial X} + \nabla^2 U \quad (6)$$

$$\frac{\partial V}{\partial \tau} + U\frac{\partial V}{\partial X} + V\frac{\partial V}{\partial Y} = -\frac{\partial P}{\partial Y} + N_{Gr}\cdot T + \nabla^2 V \quad (7)$$

$$\frac{\partial T}{\partial \tau} + U\frac{\partial T}{\partial X} + V\frac{\partial T}{\partial Y} = \frac{1}{N_{Pr}}\nabla^2 T \quad (8)$$

$$\frac{\partial U}{\partial X} + \frac{\partial V}{\partial Y} = 0 \quad (9)$$

$$\left.\begin{aligned} &U(X,Y,0) = F_1(X,Y)\\ &V(X,Y,0) = F_2(X,Y)\\ &T(X,Y,0) = -1 + 2Y\\ &T(X,0,\tau) = -1\\ &T(X,1,\tau) = 1\\ &\frac{\partial T}{\partial X}(0,Y,\tau) = \frac{\partial T}{\partial X}\left(\frac{L}{H},Y,\tau\right) = 0\\ &U = V = 0 \text{ on all surfaces.} \end{aligned}\right\} \quad (10)$$

The mean Nusselt number $N_{\overline{Nu}}$ may be expressed in terms of dimensionless variables as

$$N_{\overline{Nu}} = -\frac{1}{2}\frac{H}{L}\int_o^{L/H}\left(\frac{\partial T}{\partial Y}\right)_{Y=0} dX \quad (11)$$

The pressure terms in Equations (6) and (7) may be eliminated by subtracting the partial derivative of Equation (7) with respect to X from the partial derivative of Equation (6) with respect to Y to form

$$\frac{\partial \zeta}{\partial \tau} + U\frac{\partial \zeta}{\partial X} + V\frac{\partial \zeta}{\partial Y} = -N_{Gr}\cdot\frac{\partial T}{\partial X} + \nabla^2\zeta \quad (12)$$

where the vorticity ζ has been defined as

$$\zeta = \left(\frac{\partial V}{\partial X}\right) - \left(\frac{\partial U}{\partial Y}\right) = -\nabla^2\psi,$$

and ψ is the stream function such that

$$U = \left(\frac{\partial \psi}{\partial Y}\right);\ V = -\left(\frac{\partial \psi}{\partial X}\right).$$

Equations (12) and (8), along with the definitions of ζ and ψ, and the initial and boundary conditions

$$\left.\begin{aligned} &\psi(X,Y,0) = F(X,Y)\\ &T(X,Y,0) = -1 + 2Y\\ &T(X,0,\tau) = -1\\ &T(X,1,\tau) = 1\\ &\frac{\partial T}{\partial X}(0,Y,\tau) = \frac{\partial T}{\partial X}\left(\frac{L}{H},Y,\tau\right) = 0\\ &\psi = \frac{\partial\psi}{\partial n} = 0 \text{ on all surfaces where } n \text{ is the direction normal to the surface} \end{aligned}\right\} \quad (13)$$

constitute a condensed formal statement of the problem.

FINITE-DIFFERENCE APPROXIMATIONS

In the numerical solution of a differential equation the dependent variables are assumed to exist at a finite number of regularly spaced values of the independent variables known as *grid points*. The derivatives are then replaced by finite differences involving the values of the dependent variables at the grid points and the differential equations reduced to a series of algebraic equations which can be solved by conventional means. For the problem herein the numerical grid of Figure 2 has been used throughout.

Equations (12) and (8) are known as the *vorticity* and *energy* equations, respectively. These equations are parabolic equations because of the presence of the $\partial/\partial\tau$ term. If a solution for the ζ and T fields is known at $\tau = n\Delta\tau$ ($n = 0$ corresponds to the initial condition), then the solution at $\tau = (n+1)\Delta\tau$ may be evaluated in several ways. A two-dimensional version of the implicit, alternating direction (ADI) method introduced by Brian (4) was

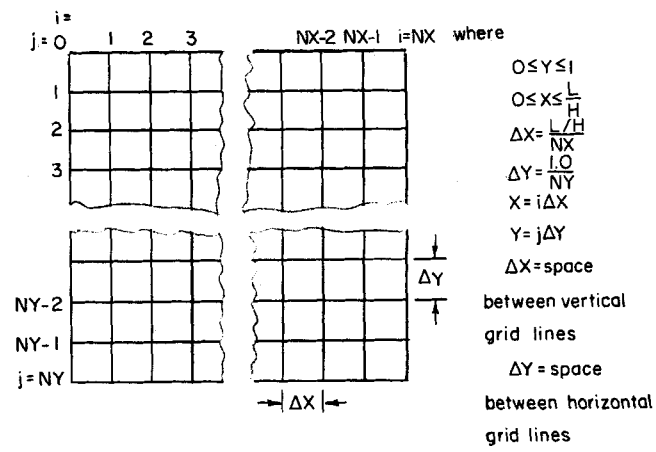

Fig. 2. The numerical grid.

used herein. For two-dimensional problems Brian's ADI method can be reduced to the usual ADI procedure. However, Brian's formulation requires slightly less computation than the usual formulation, and therefore was used in this work. When one uses Brian's procedure, the vorticity and energy equations are expressed as

Vorticity:

$$\frac{\zeta^* - \zeta^n}{\Delta\tau/2} = -N_{Gr}\,\delta_X T^{n+1} + \delta_X{}^2\,\zeta^* + \delta_Y{}^2\,\zeta^n - U\,\delta_X\zeta^* - V\,\delta_Y\zeta^n \quad (14)$$

$$\frac{2\zeta^* - \zeta^n - \zeta^{n+1}}{\Delta\tau} = \frac{1}{2}\,\delta_Y{}^2(\zeta^n - \zeta^{n+1}) - \frac{V}{2}\,\delta_Y(\zeta^n - \zeta^{n+1}) \quad (15)$$

Energy:

$$\frac{T^* - T^n}{\Delta\tau/2} = \frac{1}{N_{Pr}}\,(\delta_X{}^2\,T^* + \delta_Y{}^2\,T^n) - U\delta_X T^* - V\delta_Y T^n \quad (16)$$

$$\frac{2T^* - T^n - T^{n+1}}{\Delta\tau} = \frac{0.5}{N_{Pr}}\,\delta_Y{}^2(T^n - T^{n+1}) - \frac{V}{2}\,\delta_Y(T^n - T^{n+1}) \quad (17)$$

where central differences have been used to evaluate all first derivatives. Velocities and values of ζ at the wall are evaluated at $\tau = n\Delta\tau$ throughout the whole time step. Use of the wall vorticities and velocities in this fashion will introduce a minor error in the unsteady state results. However, since only the steady state results are considered to have significance, this error, which vanishes at steady state, was of no concern.

Once the values of ζ at $\tau = (n+1)\Delta\tau$ are known, ψ^{n+1} must be determined. When one follows the procedure of Peaceman and Rachford (*10*) the elliptic equation for the stream function is rewritten as

$$\zeta^{n+1} + \nabla^2\,\psi^{n+1} = \frac{\partial\psi^{n+1}}{\partial\tau'} \quad (18)$$

That is, the problem is converted to an unsteady problem, and numerical integration in time is carried out until the change in the ψ field becomes negligible. When the ADI procedure is used for the time integration, it is possible to use large time step sizes and, therefore, to attain the steady state rather rapidly. In most calculations only one to three iterations were required for convergence of the stream function field.

TABLE 1. SUMMARY OF CASES STUDIED

L/H	N_{Pr}	N_{Gr}
1/2	1.0	3,000, 5,000, 6,000, 7,000, 8,000, 10,000, 20,000
1/1	0.01	150,000, 170,000, 200,000, 300,000, 500,000, 1,000,000, 2,000,000, 4,000,000
1/1	0.03	50,000, 56,670, 66,670, 100,000, 167,000, 333,000, 666,700
1/1	0.1	13,000, 14,000, 15,000, 17,000, 20,000, 30,000, 50,000, 100,000, 200,000
1/1	1.0	1,300, 1,400, 1,500, 1,700, 2,000, 3,000, 5,000, 10,000, 20,000, 40,000
1/1	5.8	180, 230, 260, 360, 500, 860, 1,720
1/1	25.0	60, 75, 100, 200, 400
2/1	1.0	1,000, 1,100, 1,300, 1,500, 2,000, 3,000, 5,000, 10, 000
3/1	1.0	3,000

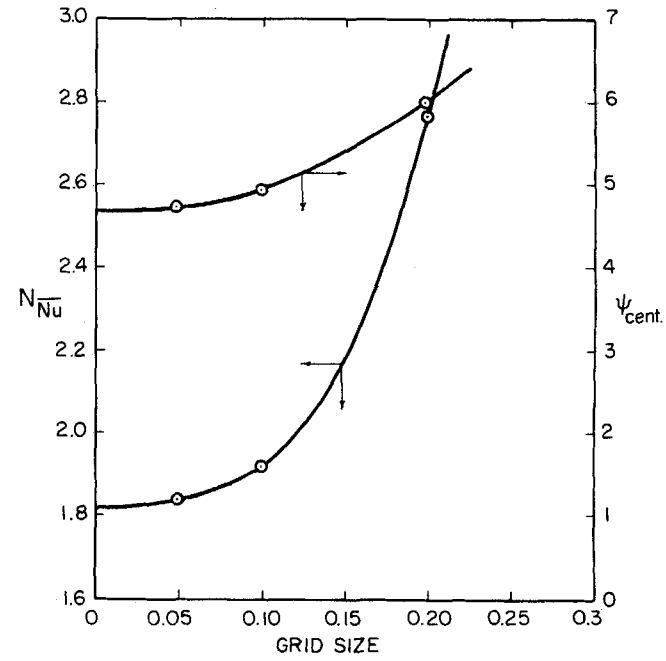

Fig. 3. Effect of grid size on steady state $N_{\overline{Nu}}$ and ψ_{cent} for a square cavity with $N_{Pr} = 1$ and $N_{Gr} = 3{,}000$.

Although Peaceman and Rachford suggested using a varying time step size for solving Equation (18), a constant step size of $\Delta\tau' = 0.04$ proved most satisfactory for $\Delta X = \Delta Y = 0.1$ and 0.05.

The following test was used to determine the convergence of the stream function iteration:

1. At the end of each iteration the vorticity $Z_{1,1}$ is calculated from the current values of ψ^{n+1}.
2. If $|(Z_{1,1} - \zeta_{1,1})/\zeta_{1,1}|$ is less than a predetermined constant *EPS*1, the iteration is assumed to have converged. If not, a new set of ψ^{n+1} is calculated, and the test is applied again.

The 1,1 point was chosen for the convergence test because early experiments indicated it was the last point to reach its final value.

Once the new field of the stream function has been calculated, the vorticities on the wall must be up dated to $\tau = (n+1)\Delta\tau$ (the wall vorticities have been held constant at their value for $\tau = n\Delta\tau$ to this point). The wall vorticity may be calculated from the new stream functions as follows.

For the wall at $X = 0$, $U = V = 0$ implies $(\partial\psi_{o,j}/\partial Y) = (\partial\psi_{o,j}/\partial X) = 0$ for all Y. $(\partial\psi_{o,j}/\partial Y)$ implies $\psi_{o,j}$ = constant for all Y, and the constant is chosen equal to 0 for convenience. Thus $(\partial^2\psi_{o,j}/\partial Y^2) = 0$ for all Y, and $\nabla^2\psi_{o,j}$ becomes $\nabla^2\psi_{o,j} = \partial^2\psi_{o,j}/\partial X^2 = -\zeta_{o,j}$. $(\partial^2{}_{o,j}/\partial X^2)$ may be calculated from the Taylor's series expansion

$$\psi_{1,j} = \psi_{o,j} + \frac{\Delta X}{1!}\,\frac{\partial\psi_{o,j}}{\partial X} + \frac{\Delta X^2}{2!}\,\frac{\partial^2\psi_{o,j}}{\partial X^2} + \cdots$$

But

$$\psi_{o,j} = \frac{\partial\psi_{o,j}}{\partial X} = 0$$

Therefore

$$-\nabla^2\,\psi_{o,j} = -\frac{2\psi_{1,j}}{\Delta X^2} = \zeta_{o,j} \quad (19)$$

Similar expressions can be derived for the other walls.

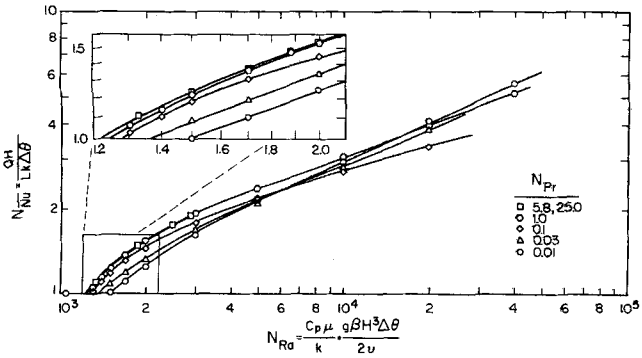

Fig. 4. Dependence of $N_{\overline{Nu}}$ on N_{Ra} and N_{Pr} for a cavity of square cross section.

Wilkes (*19*) suggests the use of a higher-order approximation to $\nabla^2\psi$, which includes $\psi_{2,j}$. However, the vorticity equation exhibited a boundary-induced instability at relatively low $\Delta\tau$ when such higher-order approximations were tested.

Four-point, central differences were used to determine U and V from ψ for points not adjacent to a boundary. Four-point, noncentral differences were used for velocities adjacent to a boundary. A four-point approximation was used to evaluate $\left(\frac{\partial T}{\partial Y}\right)_{Y=0}$ in the determination of $N_{\overline{Nu}}$.

RESULTS

To check the assumption of two-dimensional motion, an experimental program was undertaken to obtain a qualitative description of natural convection within a long, horizontal, rectangular channel heated from below. Unfortunately, the preferred mode of convection was extremely sensitive to minor perturbations in the boundary conditions, such as type of illumination, heat leakage, etc., and the equipment did not have adequate control for the desired experiments. Although interesting observations were made, they did not provide a critical test of the assumption of two-dimensional motion.

A computer program for the desired calculations was developed using the MAD (Michigan Algorithmic Decoder) language. Calculations were performed on the IBM-7090 computer at the University of Michigan Computing Center.

Calculations were performed for approximately sixty combinations of L/H, N_{Gr}, and N_{Pr}. A summary of the cases studied is presented in Table 1. In each case a set of arbitrary initial conditions (usually the results of a previous calculation) was introduced and calculations performed until $N_{\overline{Nu}}$ no longer varied significantly with time. Plots of the streamlines and isotherms which existed after the last time step were prepared by an interpolating and plotting program [see Wilkes (*19*), p. 93, for details of this program].

TABLE 2. VARIATION OF CENTRAL $\psi \cdot N_{Pr}$ AND $N_{\overline{Nu}}$ WITH N_{Pr} AT $N_{Ra} = 10{,}000$ AND $L/H = 1.0$

N_{Pr}	$N_{\overline{Nu}}$	$\psi \cdot N_{Pr}$
0.01	2.92	10.3
0.03	2.87	10.25
0.1	2.76	10.0
1.0	3.025	10.8
5.8	3.03	10.8
25.0	3.03	10.8

Grid Sizes and Numerical Stability

The effect of grid size on the steady state values of $N_{\overline{Nu}}$ and the central stream function for $N_{Ra} = 3{,}000$ is illustrated in Figure 3. The difference between the values of $N_{\overline{Nu}}$ and ψ_{cent} at $\Delta X = 0.1$ and those values extrapolated for $\Delta X = 0$ is less than 6%. For $\Delta X = 0.05$ this difference was less than 2%. Since the computing time was found to increase almost as the cube of the number of grid spaces, $\Delta X = 0.1$ was chosen as a reasonable compromise between accuracy and cost. All figures and results presented herein are for $\Delta X = 0.1$. Slightly more accurate values can be estimated on the basis of Figure 3.

For the high values of N_{Pr} and low N_{Gr}, a value of $\Delta\tau \geq 0.015$ produced numerical instabilities in the vorticity equation. Therefore $\Delta\tau = 0.01$ was used for most calculations. However, for high values of N_{Gr} and low values of N_{Pr}, $\Delta\tau$ had to be restricted further to as low as 0.0001.

In most cases about 100 to 150 time steps, which required 3 to 5 min. of computer time for a 10 × 10 grid, were needed to reach steady state.

Nusselt Number Variation with L/H, N_{Gr}, and N_{Pr}

Both Kurzweg (9) and Pellew and Southwell (*11*) found that the linearized equations of motion and energy contained only N_{Ra} as a parameter and thus implied that $N_{\overline{Nu}}$ was a function of N_{Ra} alone and not an independent function of N_{Gr} and N_{Pr}.

A plot of $N_{\overline{Nu}}$ vs. N_{Ra} for $L/H = 1.0$ and $N_{Pr} = 0.01$, 0.03, 0.1, 1.0, 5.8, and 25.0 is presented in Figure 4, from which it is apparent that for $N_{Pr} \geq 1$, $N_{\overline{Nu}} = f(N_{Ra})$ only. The linearization therefore appears justified for fluids with $N_{Pr} \geq 1$.

The dimensionless quantity $N_{Pr} \cdot \psi$, as well as $N_{\overline{Nu}}$, was found to be a function only of N_{Ra} for $N_{Pr} \geq 1$. Since

$$N_{Pr} \cdot \psi = \int_o^Y U dY = \kappa \int_o^y u dy \qquad (20)$$

$$N_{Pr} \cdot \psi = \int_o^X V dX = \kappa \int_o^x v dx \qquad (21)$$

it follows that the dimensional velocities u and v are dependent only on the Rayleigh number and thermal diffusivity when $N_{Pr} \geq 1$.

For $N_{Pr} < 1$, $N_{\overline{Nu}}$ is seen to exhibit a marked dependence on N_{Pr} as well as on N_{Ra}. $\psi \cdot N_{Pr}$ also varies with

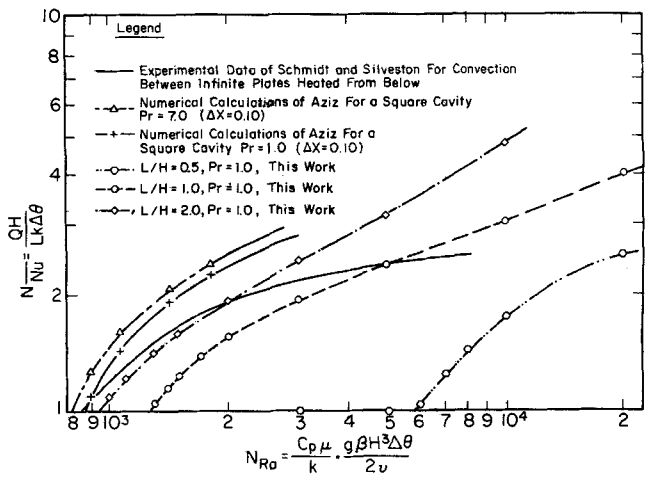

Fig. 5. Comparison of the results of this investigation with the calculations of Aziz and the data of Schmidt and Silveston.

N_{Pr} for small N_{Pr} as indicated in Table 2. This variation of $N_{\overline{Nu}}$ and $\psi \cdot N_{Pr}$ with N_{Pr} indicates that the linearization is not valid for $N_{Pr} < 1$.

The results of Aziz were found to be much more strongly dependent on the grid size than those of the investigation reported herein. The reason for this greater truncation error is not apparent. When Aziz' results for different grid size were extrapolated to zero grid size, good agreement was obtained with the results of this investigation. However, Aziz presented values for different grid size for only two values of N_{Ra}, at $N_{Pr} = 1.0$. The values of N_{Ra} that he presents for $\Delta X = 0.10$ are significantly higher than values obtained by the extrapolation to zero grid size, and indicate a critical value of N_{Ra} that is considerably lower than values determined herein and by Kurzweg.

The results of Aziz for two-dimensional convection in a square region (with $\Delta X = 0.1$) are compared in Figure 5 with the results of this investigation, and with the experimental results of Schmidt and Silveston, for convection between two essentially infinite, flat plates. The critical value of N_{Ra} produced by extrapolating Aziz' results for $N_{\overline{Nu}}$ to unity is even lower than the experimental value for convection between infinite plates, which is clearly inconsistent. Extrapolation to zero grid size would have eliminated this inconsistency.

Determination of the Critical Rayleigh Number

The critical Rayleigh number was determined herein by extrapolating a plot of $N_{\overline{Nu}}$ vs. N_{Ra} to $N_{\overline{Nu}} = 1.0$ (pure conduction). Below N_{Ra_c}, $N_{\overline{Nu}}$ equaled 1.0 independent of N_{Ra}. The critical N_{Ra} for the various cases studied are presented in Table 3 along with the results of Kurzweg (9), who used the linearized equations of motion to pre-

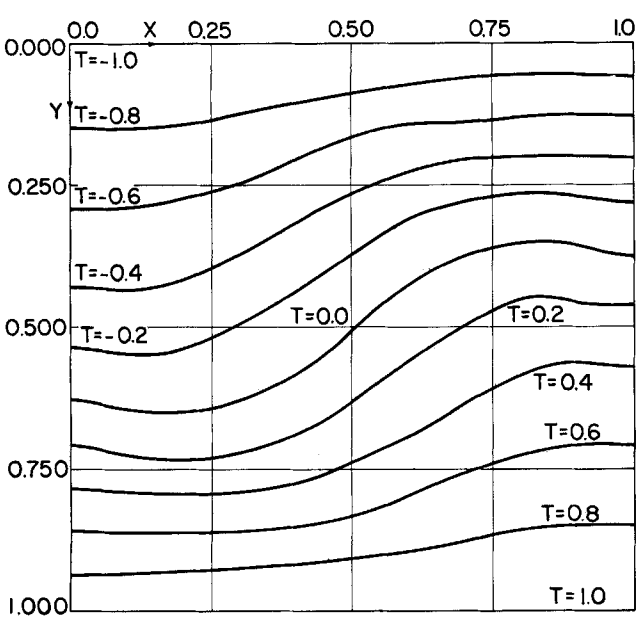

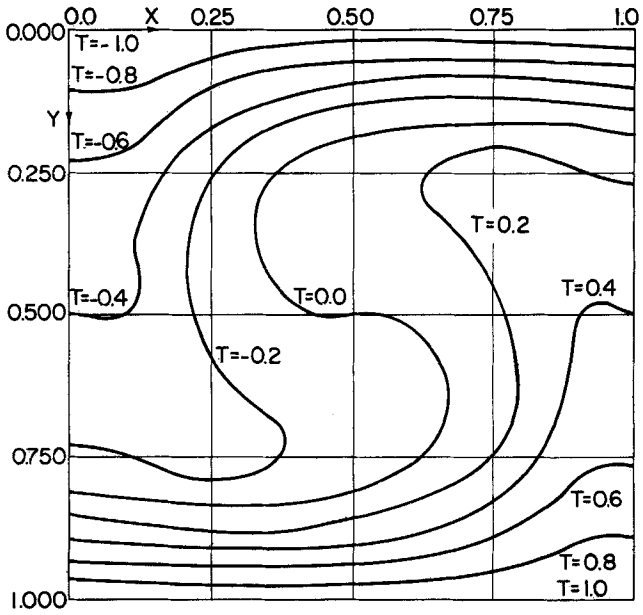

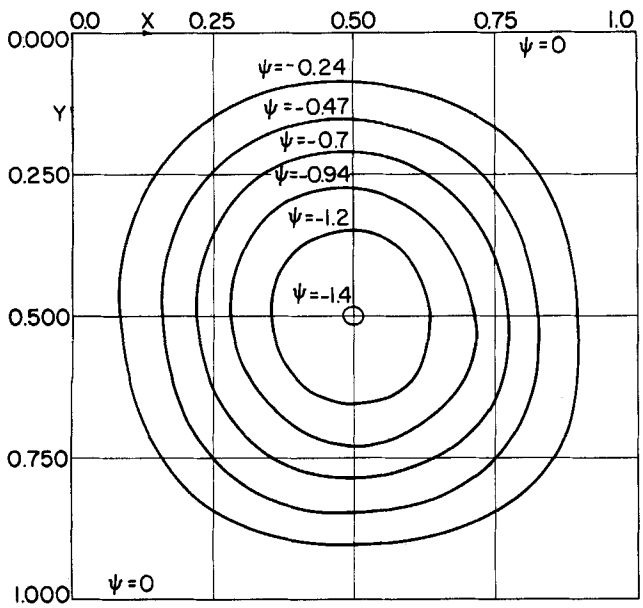

Fig. 6. Steady state streamlines and isotherms for $L/H = 1.0$, $N_{Pr} = 1.0$, and $N_{Gr} = 1{,}400$.

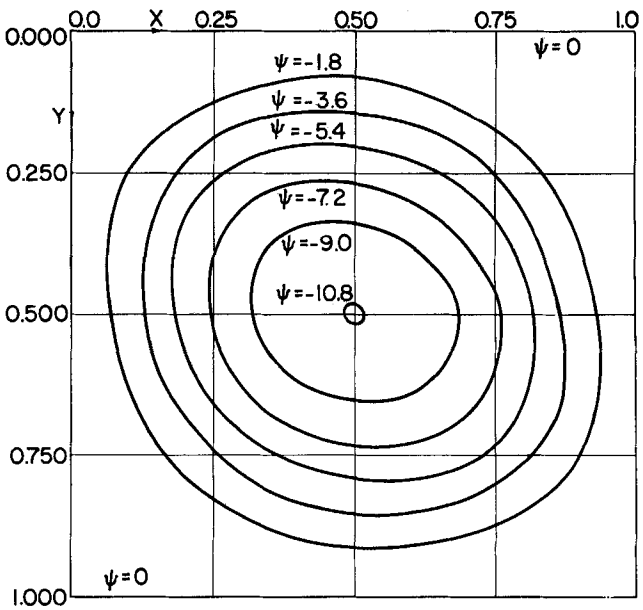

Fig. 7. Steady state streamlines and isotherms for $L/H = 1.0$, $N_{Pr} = 1.0$, and $N_{Gr} = 10{,}000$.

dict the critical N_{Ra}. Comparison of Kurzweg's results with those of this investigation indicates good agreement for $N_{Pr} \geq 1$. However, for $N_{Pr} < 1$, a significant variation of N_{Ra_c} with N_{Pr} was found and confirms the previous observation that linearization is not justifiable for low N_{Pr}.

Streamline and Isotherm Plots

In Figures 6 to 9 streamlines and isotherms are plotted for several values of L/H, N_{Gr}, and N_{Pr}. In Figures 6 and 7 the build-up of convective strength is observed as the N_{Ra} increases in a square cavity with $N_{Pr} = 1$. At low N_{Ra} the isotherms are almost straight, equally spaced, horizontal lines, while the streamlines are nearly circular. As N_{Ra} increases, the isotherms become increasingly distorted

Table 3. Critical N_{Ra} as a Function of L/H and N_{Pr}

L/H	N_{Pr}	N_{Ra_c} This work	N_{Ra_c} Kurzweg	N_{Ra_c} Aziz
2/1	1.0	920	1,008	
1/1	0.01	1,500		
1/1	0.03	1,380		
1/1	0.10	1,270		
1/1	1.0	1,240	1,290	850
1/1	5.8	1,230		
1/1	7.0			750
1/1	25.0	1,230		
1/2	1.0	5,800	6,060	

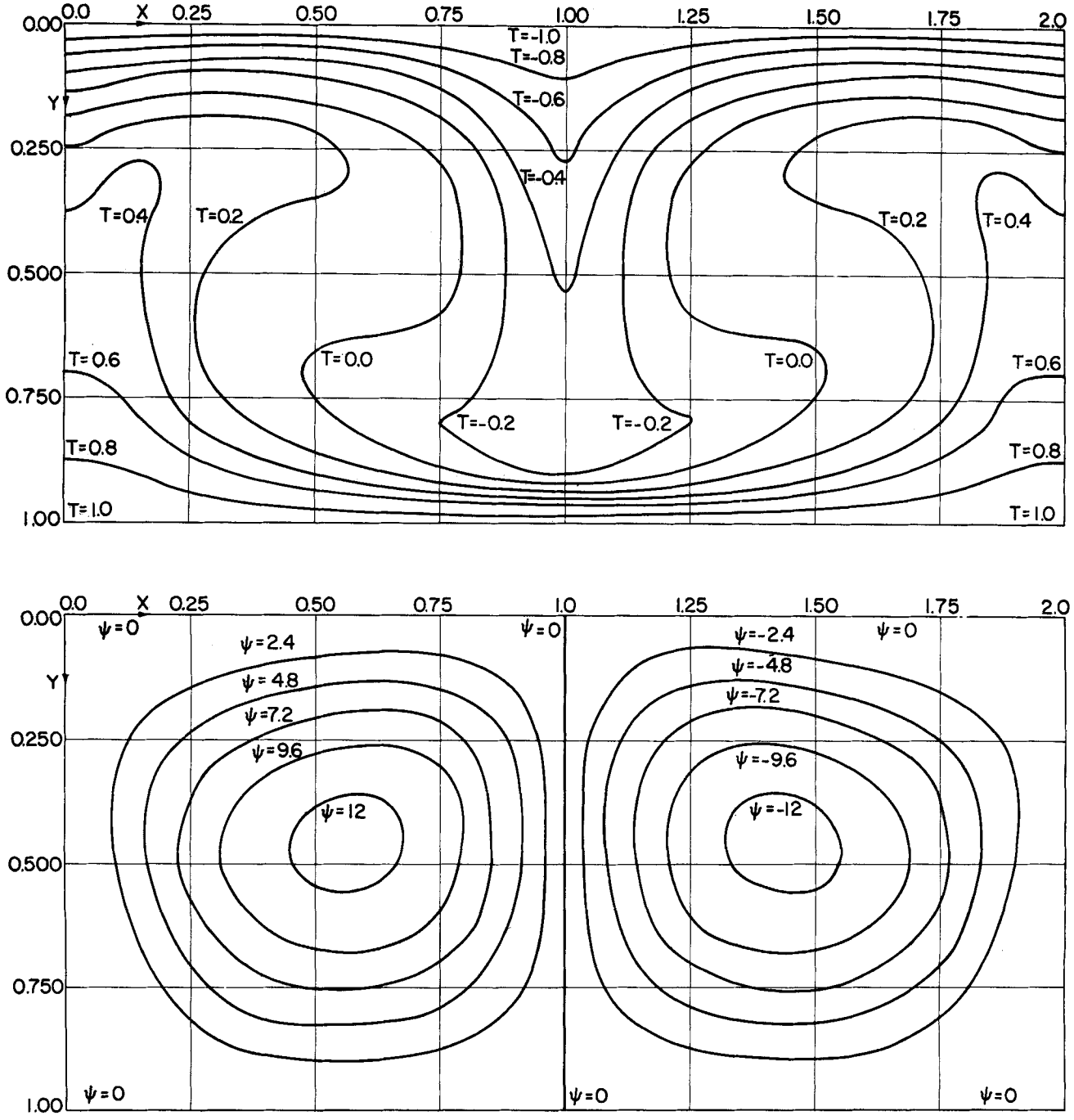

Fig. 8. Steady state streamlines and isotherms for $L/H = 2$, $N_{Pr} = 1.0$, and $N_{Gr} = 10{,}000$.

as a nearly isothermal core with $-0.2 \leq T \leq +0.2$ develops. In the core, conduction is almost negligible and convection is responsible for the major portion of the heat transfer. As N_{Ra} increases the size of the core region also increases. The streamlines, on the other hand, have distorted only slightly into an oblong shape. It was noted that a region of separated flow had developed in several cases. The coarseness of the numerical grid prevented a description of the separated region. However, the occurrence of this separated region did not appear to have a significant effect on the heat transfer rates.

In Figures 8 and 9 streamlines and isotherms are presented for $L/H = 2/1$ and $3/1$. The existence of multicelled patterns should be noted. For a cavity with $L/H = 2/1$ and $N_{Pr} = 1$, a series of cases with varying N_{Ra} was studied. The heat transfer rates are presented in Figure 5, which indicates the similarity, in the region of the critical Rayleigh number, between the two-dimensional calculations for $L/H = 2/1$ and the experimental values of Schmidt and Silveston for convection between infinite plates. (It is expected that $L/H = 3/1, 4/1 \ldots$ will produce better and better agreement with the experimental values in the region of N_{Ra_c}.) This close agreement may well indicate the presence of two-dimensional cells in the experimental work for values of N_{Ra} near N_{Ra_c}.

Preferred Mode of Natural Convection

Fromm (7) found that two-, three-, and four-celled patterns can exist in a region with $L/H = 7/3$, if symmetrical initial conditions are used as a starting disturbance. However, the use of symmetrical initial conditions appears artificial, since any real motion would undoubtedly be generated by some form of nonsymmetrical disturbance. Therefore, it was desirable to determine what configuration would result if two-, three-, or four-celled patterns with the same L/H were subjected to an unsymmetrical disturbance.

To test the effect of initial conditions, unsymmetrical one- and two-celled initial conditions were applied to regions with L/H equal to 1.0 and 2.0. For the $L/H = 1.0$ cell both sets of initial conditions produced an identical steady state with one cell. For the $L/H = 2$ region both sets of initial conditions produced identical steady states with two cells. Thus when nonsymmetrical initial conditions are used, the steady state is independent of the initial conditions. However, when symmetrical one- and three-celled patterns were used in the $L/H = 2.0$ region, one- and three-celled patterns, respectively, were found at steady state.

Finally a one-cell disturbance was placed in the upper left-hand corner of a quiescent region with $L/H = 3.0$. As time progressed, two, three, four, and then three cells were present. The final pattern consisted of three cells that were symmetrical about the centerline of the cavity as illustrated in Figure 9.

Symmetrical initial conditions were then used to generate one-, two-, and three-celled patterns in a region with $L/H = 2.0$. When the three patterns were subjected to a nonsymmetrical disturbance, the final steady patterns were always two-celled. In all cases the steady state

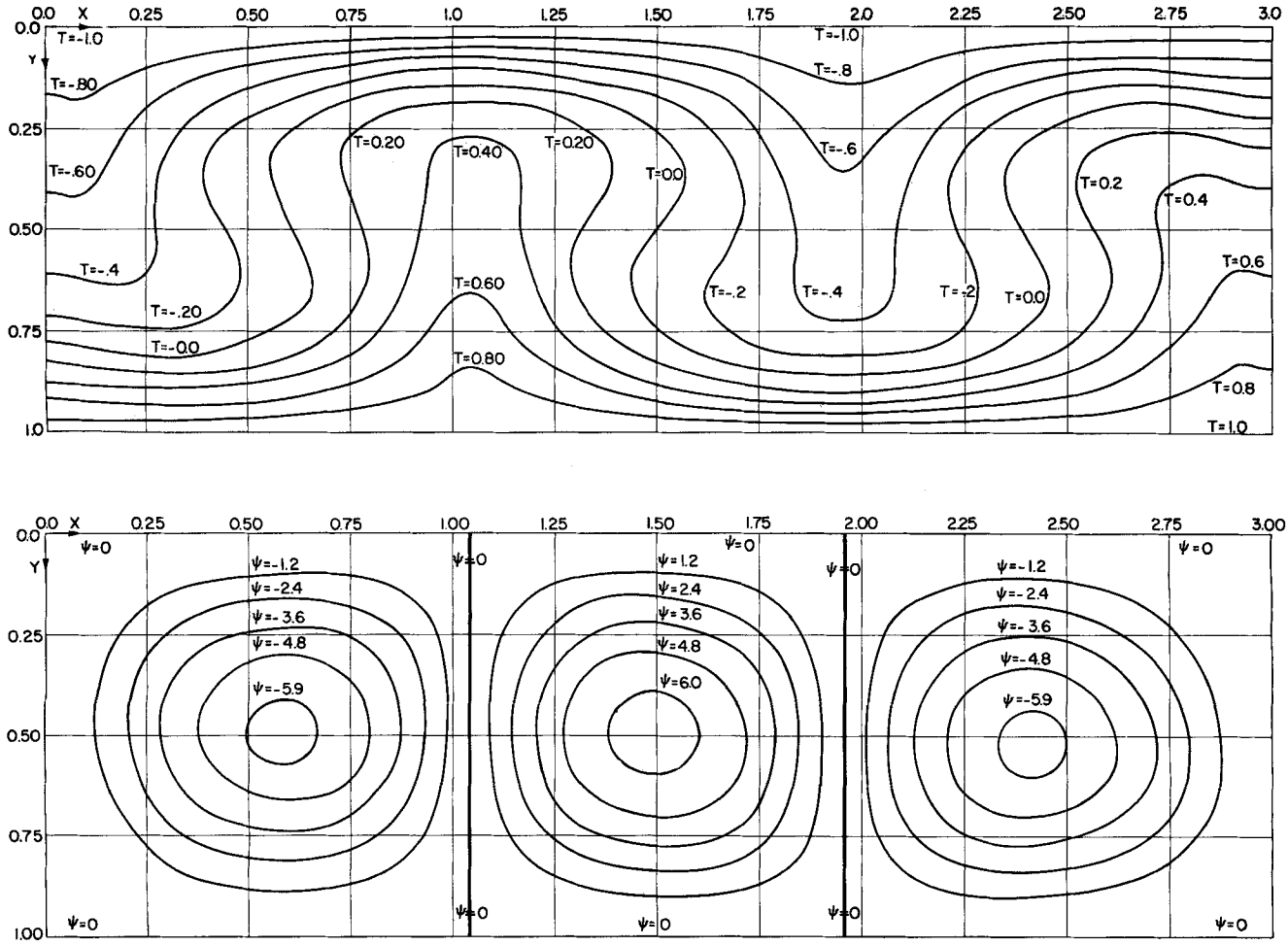

Fig. 9. Steady state streamlines and isotherms for $L/H = 3$, $N_{Pr} = 1.0$, and $N_{Gr} = 3{,}000$.

streamlines and isotherms were identical to those found when a symmetrical, or nonsymmetrical, two-celled pattern was used as the initial condition.

These tests are not absolutely conclusive, since the effects of different forms of disturbance and of the magnitude of the disturbance were not investigated. However, the results do suggest that although many cellular arrangements can be forced to occur in any given cavity, only that arrangement in which the number of cells is equal to L/H (for integral values of L/H) will be stable to a general nonsymmetrical disturbance, and hence is the preferred mode.

SUMMARY

The applicability of finite-difference techniques in the determination of hydrodynamic stability has been demonstrated. In particular, natural convection in an enclosed horizontal region of rectangular cross section which is heated from below was studied. Critical Rayleigh numbers were determined and compared with those analytically determined by Kurzweg. Excellent agreement was found for those cases where $N_{Pr} \geq 1$.

ACKNOWLEDGMENT

The authors thank the National Science Foundation, whose financial support made this work possible.

NOTATION

c_p = heat capacity at constant pressure, B.t.u./(lb.$_m$) (°F.)
$f(x,y)$ = initial velocity conditions for integration of momentum equation, ft./hr.
$F(X,Y)$ = initial condition for integration of the dimensionless momentum or vorticity equation
g = acceleration of gravity, ft./sec.^{2}
H = height of cell, ft.
k = thermal conductivity, B.t.u./(hr.) (ft.) (°F.)
L = length of cell, ft.
$N_{Gr} = \dfrac{H^3 g\beta\Delta\theta}{2\nu^2}$, Grashof number based on ½ temperature difference, dimensionless
$N_{\overline{Nu}} = QH/Lk\Delta\theta$, mean Nusselt number, dimensionless
$N_{Pr} = c_p\mu/k$, Prandtl number, dimensionless
$N_{Ra} = N_{Gr} \cdot N_{Pr}$, Rayleigh number based on ½ temperature difference, dimensionless
N_{Rac} = critical Rayleigh number for onset of convection
NX = number of vertical grid spaces
NY = number of horizontal grid spaces
p = pressure, lb.$_f$/sq.ft.
$P = pH^2/\rho\nu^2$, dimensionless pressure
Q = total heat transferred per unit of cavity depth B.t.u./(hr.) (ft.)
t = time, hr.
$T = 2(\theta - \theta_o)/(\theta_h - \theta_l)$, dimensionless temperature
u = velocity in x direction, ft./hr.
$U = uH/\nu$, dimensionless velocity in X direction
v = velocity in y direction, ft./hr.
$V = vH/\nu$, dimensionless velocity in Y direction
x = horizontal coordinate, ft.
$X = x/H$, dimensionless horizontal coordinate
y = vertical coordinate, ft.
$Y = y/H$, dimensionless vertical coordinate

Greek Letters

$\Delta X = \dfrac{L}{H}/NX$, grid spacing in X direction
$\Delta Y = 1/NY$, grid spacing in Y direction
$\Delta\theta = \theta_h - \theta_l$, temperature difference between upper and lower surfaces of cavity
$\Delta\tau$ = dimensionless time step size
$\nabla^2 = \dfrac{\partial^2}{\partial X^2} + \dfrac{\partial^2}{\partial Y^2}$, Laplacian operator, dimensionless
δ_X = central finite-difference approximation to $\partial/\partial X$
$\delta_X{}^2$ = central finite-difference approximation to $\partial^2/\partial X^2$
$\zeta = -\nabla^2\psi$, dimensionless vorticity
θ = temperature, °F.
$\kappa = c_p\rho/k$, thermal diffusivity, sq.ft./hr.
$\nu = \mu/\rho$, kinematic viscosity, sq.ft./hr.
ρ = density, lb.$_m$/cu.ft.
$\tau = \nu t/H^2$, dimensionless time
ψ = dimensionless stream function, such that $U = \partial\psi/\partial Y$, $V = -\partial\psi/\partial X$

Subscripts

cent = central
h = high
i = i^{th} grid point
j = j^{th} grid point
l = low
o = evaluated at the mean temperature, $(\theta_h + \theta_l)/2$

Superscripts

n = n^{th} time step
$\overline{\ }$ = mean value
$'$ = stream function iteration

LITERATURE CITED

1. Aziz, Khalid, Ph.D. thesis, Rice Univ., Houston, Tex. (1965).
2. Baraket, H. Z., Ph.D. thesis, Univ. Michigan, Ann Arbor (1965).
3. Bénard, Henri, *Rev. Gen. Sci. Pures Appl.*, **11**, 1261, 1309 (1900).
4. Brian, P. L. T., *A.I.Ch.E. J.*, **7**, 367 (1961).
5. Deardorff, J. W., *J. Atm. Sci.*, **21**, 149 (1954).
6. Fromm, J. E., *Los Alamos Sci. Lab. Rept. No. La-2910* (1963).
7. ———, *Phys. Fluids*, **8**, 1757 (1965).
8. Hellums, J. D., and S. W. Churchill, *Chem. Eng. Progr. Symposium Ser. No. 32*, **57**, 75 (1961).
9. Kurzweg, U. H., *Intern. J. Heat Mass Transfer*, **8**, 35 (1965).
10. Peaceman, D. W., and H. H. Rachford, *J. Soc. Ind. Appl. Math.*, **3**, No. 1, 28 (1955).
11. Pellew, Anne, and R. V. Southwell, *Proc. Roy. Soc. London*, **A176**, 312 (1940).
12. Poots, G., *Quart. Mech. Appl. Math.*, **11**, 257 (1958).
13. Rayleigh, J. W. S., *Phil. Mag.*, **32**, 529 (1916).
14. Samuels, M. R., Ph.D. thesis, Univ. Michigan, Ann Arbor (1965).
15. Schmidt, Ernst, and P. L. Silveston, *Chem. Eng. Progr. Symposium Ser. No. 29*, **55**, 163 (1959).
16. Sorokin, M. P., *Inzh. Fiz. Zh.*, **4**, No. 8, 107 (1961).
17. Sternling, C. V., and L. E. Scriven, *J. Fluid Mech.*, **19**, 321 (1964).
18. Thomson, J. J., *Proc. Glasgow Phil. Soc.*, **13**, 464 (1882).
19. Wilkes, J. O., Ph.D. thesis, Univ. Michigan, Ann Arbor (1963).
20. ———, and S. W. Churchill, *A.I.Ch.E. J.*, **12**, 161 (1966).

Manuscript received April 7, 1966; revision received July 11, 1966; paper accepted July 11, 1966. Paper presented at A.I.Ch.E. Atlantic City meeting.